Atmos. Chem. Phys. Discuss., 15, 33077–33119, 2015
www.atmos-chem-phys-discuss.net/15/33077/2015/
doi:10.5194/acpd-15-33077-2015

Atmospheric Chemistry and Physics Discussions
Open Access

High concentrations of sub-3 nm clusters and frequent new particle formation observed in the Po Valley, Italy, during the PEGASOS 2012 campaign

J. Kontkanen[1], E. Järvinen[1,2], H. E. Manninen[1], K. Lehtipalo[1,3], J. Kangasluoma[1], S. Decesari[4], G. P. Gobbi[5], A. Laaksonen[6,7], T. Petäjä[1], and M. Kulmala[1]

[1]Department of Physics, 00014 University of Helsinki, Helsinki, Finland
[2]Institute for Meteorology and Climate Research, Karlsruhe Institute of Technology, 76021 Karlsruhe, Germany
[3]Paul Scherrer Institute, 5232 Villigen PSI, Switzerland
[4]Istituto di Scienze dell'Atmosfera e del Clima, CNR, 40129 Bologna, Italy
[5]Institute of Atmospheric Sciences and Climate, CNR, 00133 Rome, Italy
[6]Department of Applied Physics, University of Eastern Finland, 70211 Kuopio, Finland
[7]Finnish Meteorological Institute, 00101 Helsinki, Finland

High concentrations of sub-3 nm clusters and frequent new particle formation

J. Kontkanen et al.

Received: 25 September 2015 – Accepted: 9 November 2015 – Published: 24 November 2015

Correspondence to: J. Kontkanen (jenni.kontkanen@helsinki.fi)

Published by Copernicus Publications on behalf of the European Geosciences Union.

Abstract

The concentrations of neutral and charged sub-3 nm clusters and their connection to new particle formation (NPF) were investigated during the PEGASOS campaign (7 June–9 July 2012) at the San Pietro Capofiume measurement station in the Po Valley, Italy. Continuous high concentrations of sub-3 nm clusters were detected during the measurement period, although the condensation sink was relatively high (median value $1.1 \times 10^{-2}\,s^{-1}$). The median cluster concentrations were 2140 and 7980 cm^{-3} in the size bins of 1.5–1.8 nm and 1.8–3 nm, and the majority of them were electrically neutral. NPF events were observed during the measurement period frequently, on 86 % of the days. The median growth rates of clusters during the events were 4.3, 6.0 and 7.2 $nm\,h^{-1}$ in the size ranges of 1.5–3, 3–7 and 7–20 nm. The median formation rate of 1.6 nm clusters was high, 45 $cm^{-3}\,s^{-1}$, and it exceeded the median formation rate of 2 nm clusters by one order of magnitude. The ion-induced nucleation fraction was low; the median values were 0.7 % at 1.6 nm and 3.0 % at 2 nm. On NPF event days the neutral cluster concentration had a maximum around 9 a.m. (local winter time), which was absent on a non-event day. The increase in the cluster concentrations in the morning coincided with the increase in the boundary layer height. At the same time radiation and temperature increased and RH and condensation sink decreased. The concentration of neutral clusters was observed to have a positive correlation with sulfuric acid proxy, indicating the significance of sulfuric acid for the cluster formation in San Pietro Capofiume. The condensation sink had a negative correlation with the concentration of charged clusters but no clear relation to the neutral cluster concentration. This finding, together with back-trajectory analysis, suggests that the precursor vapors of the clusters and background aerosol particles, acting as their sink, have possibly originated from the same sources, including e.g. power plants and industrial areas in the Po Valley.

ACPD
15, 33077–33119, 2015

1 Introduction

New particle formation (NPF) is a dominant source of aerosol particles in the atmosphere (Spracklen et al., 2006; Yu et al., 2010). The process takes place by the formation of nanometer-sized atmospheric clusters and their subsequent growth to larger particles (Kulmala et al., 2007, 2013). After that they may affect the climate through indirect radiative effects of aerosol particles (Merikanto et al., 2009; Wang and Penner, 2009; Kazil et al., 2010; Makkonen et al., 2012). NPF has been observed around the world in various locations (Kulmala et al., 2004a; Zhang et al., 2012). Although recent chamber studies have provided insight into the role of different chemical compounds in NPF (Kirkby et al., 2011; Almeida et al., 2013; Schobesberger et al., 2013; Riccobono et al., 2014), the exact mechanisms, by which the process takes place in different ambient conditions, are still unknown. The summary of the recent knowledge on physical and chemical processes behind NPF is given by Kulmala et al. (2014).

The relative importance of electrically neutral and charged clusters in atmospheric NPF has been under discussion for decades. Some model studies underline the importance of ions (Yu and Turco, 2000, 2008), while field measurements conducted with ion spectrometers suggest only minor contribution of ions to NPF in the continental boundary layer (Iida et al., 2006; Kulmala et al., 2007; Manninen et al., 2010) and also higher in the troposphere (Mirme et al., 2010). Recent instrumental development has enabled measuring the concentrations of sub-3 nm particles also with condensation particle counters, including a Particle Size Magnifier (PSM; Vanhanen et al., 2011). With these measurement techniques, it has been observed that sub-3 nm neutral clusters exist in boreal forest (Lehtipalo et al., 2009; Kulmala et al., 2013), in coastal areas (Lehtipalo et al., 2010), and at high altitude in the free tropospheric conditions (Rose et al., 2015). At all these sites, the concentrations of neutral clusters clearly exceed ion concentrations during NPF, which indicates that neutral nucleation mechanisms dominate in these environments. Furthermore, high concentrations of sub-3 nm clusters during NPF events have been detected with a PSM at urban sites in the United States

ACPD
15, 33077–33119, 2015

(Yu et al., 2014) and at urban, heavily polluted, sites in China (Xiao et al., 2015; Yu et al., 2015).

In many of the earlier studies, sub-3 nm clusters detected with a PSM have been observed to be associated with elevated sulfuric acid concentration (Kulmala et al., 2013; Yu et al., 2014). This indicates that sulfuric acid is a key compound in the formation of atmospheric clusters, as has been proposed already earlier (e.g. Weber et al., 1997; Sipilä et al., 2010). Sulfuric acid is formed in the atmosphere by the oxidation of sulfur dioxide (SO_2), which is largely produced in fossil fuel combustion. Therefore, anthropogenic emissions of SO_2 may enhance the formation of sub-3 nm clusters. On the other hand, high aerosol surface area related to anthropogenic emissions may reduce the sub-3 nm cluster concentrations by coagulation (Kerminen et al., 2001; Xiao et al., 2015). Besides sulfuric acid, organic compounds with very low volatility may participate in atmospheric cluster formation (Kulmala et al., 1998; Metzger et al., 2010; Ehn et al., 2014; Schobesberger et al., 2013; Riccobono et al., 2014). These compounds are formed in the atmosphere in the oxidation of VOCs (volatile organic compounds), mainly originating from biogenic sources, such as vegetation (Günther et al., 2012).

In addition to the concentrations of low-volatile precursor vapors, meteorological conditions may influence the sub-3 nm cluster concentrations. Local meteorology can affect cluster concentrations in several ways. For instance, solar radiation drives oxidation mechanisms forming low-volatile vapors, which, as mentioned above, may participate in the formation of clusters. This is indicated by numerous observations on the importance of solar radiation for NPF (e.g. Boy et al., 2002; Nieminen et al., 2015). In addition, NPF has been observed to be more favorable when relative humidity and background aerosol concentrations are low (Hyvönen et al., 2005; Hamed et al., 2011; Nieminen et al., 2015). It has also been proposed that the beginning of NPF may be linked to the onset of turbulence in the boundary layer (Nilsson et al., 2001a). In addition, the origin of air masses has been connected to the probability of NPF events in several locations (Nilsson et al., 2001b; Sogacheva et al., 2007; Nieminen et al., 2015).

In this study, we investigated the concentrations of sub-3 nm clusters at the San Pietro Capofiume station located in the Po Valley, Italy, during the PEGASOS campaign (7 June–9 July 2012). Previously, NPF events have been found to be frequent in San Pietro Capofiume during summer (Laaksonen et al., 2005; Hamed et al., 2007; Manninen et al., 2010), which may be due to the high emissions of anthropogenic precursor vapors and favorable meteorological conditions. Here, our aim is to further investigate NPF occurring at this site focusing on the concentrations of sub-3 nm clusters and their connection to NPF events. Furthermore, we aim to elucidate the effect of meteorological conditions and the presence of anthropogenic pollutants on the sub-3 nm cluster concentrations in San Pietro Capofiume. During the campaign, the concentration of all sub-3 nm clusters were measured with a PSM and the concentration of charged clusters with a NAIS (Neutral cluster and Air Ion Spectrometer; Kulmala et al., 2012). From these measurements, we determined the growth rates and formation rates of clusters. We compared the diurnal variation of cluster concentrations and their formation rates to the diurnal evolution of planetary boundary layer and the variation of different meteorological variables. In addition, we studied how sulfuric acid concentration and condensation sink as well as the origin of air masses affect the concentrations of sub-3 nm clusters observed in San Pietro Capofiume.

2 Measurements and data analysis

2.1 Site description and instrumentation

The measurements took place at the San Pietro Capofiume meteorological station in northern Italy (44°39′ N, 11°37′ E, 11 m a.s.l.) during 7 June–9 July 2012. The measurements were part of the PEGASOS (Pan-European Gas–Aerosol–Climate Interaction Study) Zeppelin campaign where San Pietro Capofiume was one of the ground stations. The meteorological station is located about 30 km northeast from the city of Bologna in the Po Valley. The Po Valley region is situated between the Alps in the north

Discussion Paper | Discussion Paper | Discussion Paper | Discussion Paper |

ACPD

15, 33077–33119, 2015

High concentrations of sub-3 nm clusters and frequent new particle formation

J. Kontkanen et al.

and the Apennines Mountains in the south-southwest. The mountains surround the valley on three sides and strongly modify both the local and regional air flow patterns in the area (Sogacheva et al., 2007). High levels of anthropogenic pollutants have been observed in the region due to the emissions from power plants and industrial areas. In addition, the emissions from ship traffic in the Adriatic Sea (Hamed et al., 2007) and long-range transport from Central and Eastern Europe are possible sources of pollutants in the region (Sogacheva et al., 2007).

During the measurement campaign, the total particle concentrations were measured with an Airmodus Particle Size Magnifier (PSM A09; Vanhanen et al., 2011). PSM is a dual-stage mixing-type condensation particle counter. In the first stage, diethylene-glycol is used to activate and grow the particles to about 90 nm in diameter, after which the further growth and the counting of particles is done with a conventional CPC. The cut-off size of the PSM can be changed by altering the mixing ratio of the sample and saturator flow. In this study, the cut-off sizes of 1.5 and 1.8 nm were used, and thus, the total concentration of clusters in the size range of 1.5–1.8 nm was obtained. In addition, a twin-DMPS (Differential Mobility Particle Sizer) system was used to measure the number size distribution of all particles larger than 3 nm (Aalto et al., 2001). By subtracting the concentration measured with the highest cut-off size of the PSM from the total particle concentration measured with the DMPS, we obtained the total concentration of clusters and particles in the size range of 1.8–3 nm. Furthermore, the number size distributions of positive and negative ions between 0.8 and 42 nm and the number size distributions of all particles between 2 and 42 nm were measured with a Neutral Cluster and Air Ion Spectrometer (NAIS; Kulmala et al., 2012; Mirme and Mirme, 2013). By interpolating the NAIS data, the ion concentrations in the 1.5–1.8 nm and 1.8–3.0 nm size ranges were obtained. However, the NAIS was not working properly in ion mode during 11–21 June, and therefore this period was excluded from the analysis.

In addition to particle size distribution data, SO_2 concentration and meteorological data, including temperature, relative humidity and global radiation, measured at the station were used in the analysis. Furthermore, the measurement station was equipped

ACPD
15, 33077–33119, 2015

with a ceilometer (Jenoptik CHM15K), which allowed us to monitor the evolution of planetary boundary layer (PBL; Di Giuseppe et al., 2012; Angelini and Gobbi, 2014).

2.2 Determining the concentration of neutral clusters

To study the importance of ion-mediated processes for cluster formation, we calculated the number of neutral clusters originating from the collisions between oppositely charged ions, i.e. recombination products, in the size bins of 1.5–1.8 nm and 1.8–3 nm. The concentration of recombination products in size bin i was obtained from (Kontkanen et al., 2013):

$$N_{\mathrm{rec},i} = \frac{\lambda_i \alpha \sum_{j,k} r_{ijk} N_j^+ N_k^-}{\mathrm{CoagS}_i}. \quad (1)$$

Here λ_i represents the fraction of stable recombination products that do not break up instantly after their formation in size bin i. α is the ion–ion recombination coefficient for which we used the value of $1.6 \times 10^{-6}\,\mathrm{cm^3\,s^{-1}}$ (Hoppel and Frick, 1986; Tammet and Kulmala, 2005). N_j^+ and N_k^- refer to the concentrations of positive and negative ions in size ranges j and k, respectively, and r_{ijk} tells how large fraction of the recombination products formed in their collisions end up in size bin i. CoagS_i is the average coagulation sink for size range i. Thus, Eq. (1) takes into account the production of neutral clusters in the collisions between two oppositely charged ions (the term in the numerator) and their loss by coagulation (the term in the denominator). The effect of the condensational growth of clusters was neglected, as has been done in most of the earlier studies discussing the concentrations of recombination products (e.g. Lehtipalo et al., 2009; Kulmala et al., 2013). The production rate of neutral clusters due to ion-ion recombination was calculated from the ion size distribution measured with the NAIS. For the detailed description of the procedure, see Kontkanen et al. (2013). The fraction of stable recombination products, λ_i, was assumed to equal unity. The coagulation loss

ACPD
15, 33077–33119, 2015

of clusters because of their collisions onto larger aerosol particles was calculated from DMPS data (Kulmala et al., 2001).

After calculating the concentration of recombination products, we calculated the concentration of neutral clusters ($N_{n,i}$), not originating from ion-ion recombination (from now on we refer to these as just neutral clusters), in the size bins of 1.5–1.8 nm and 1.8–3 nm by subtracting the concentrations of ions ($N_{ions,i}$) and recombination products ($N_{rec,i}$) from the total cluster concentration ($N_{tot,i}$):

$$N_{n,i} = N_{tot,i} - N_{ions,i} - N_{rec,i} \quad (2)$$

For calculating the concentration of neutral clusters from Eq. (2) 10 min averaged data from the NAIS ($N_{ions,i}$), and from the PSM and the DMPS ($N_{tot,i}$) were used.

2.3 New particle formation event analysis

The classification of measurement campaign days into new particle formation (NPF) event days and non-event days was done by visually evaluating ion size distribution data from the NAIS (Dal Maso et al., 2005; Hirsikko et al., 2007). The days when new particle formation and growth were observed were classified as NPF event days, while the days with no implication of NPF were assigned as non-event days.

The growth rates of 1.5–3, 3–7 and 7–20 nm particles were determined for the identified NPF events. For calculating the growth rates, we used positive ion size distribution data measured with the NAIS and applied the method by Hirsikko et al. (2005). In this method a Gaussian distribution is fitted to the concentration time series at a certain size to determine the moment of maximum concentration. Then, the growth rate is obtained as the slope of a linear least square fit to the moments of maximum concentrations and the corresponding geometric mean diameters of the particles. For the comparison of particle growth rates determined using different instruments and methods, see Yli-Juuti et al. (2011).

The total particle formation rates and ion formation rates at 1.6 nm ($J_{1.6}$) and at 2 nm (J_2) were calculated following the method in Kulmala et al. (2012). When calculating the total particle formation rate, we determined the time derivative of particle concentration and took into account the effects of coagulation loss and the growth out of the studied size range. The accuracy of this method is evaluated in Korhonen et al. (2011). When determining the ion formation rate, the loss of ions by ion-ion recombination and the charging of neutral particles were also included in the calculation. The total particle formation rate at 1.6 nm was determined from the PSM data, while for calculating the total particle formation rate at 2 nm we used NAIS particle size distribution data. The ion formation rates were calculated from the NAIS ion size distributions. For the growth rates needed for the calculations, we used the growth rates determined for 1.5–3 nm size range from the NAIS data.

2.4 Sulfuric acid proxy

To study the connection between the concentrations of sub-3 nm clusters and sulfuric acid, we calculated the sulfuric acid concentration from a non-linear statistical proxy derived by Mikkonen et al. (2011):

$$SA_{proxy} = 8.21 \times 10^{-3} \times k \times \mathrm{Rad} \times [SO_2]^{0.62} \times (\mathrm{CS} \times \mathrm{RH})^{-0.13} \quad (3)$$

Here k describes the reaction rate coefficient, which depends on air temperature and atmospheric pressure. Rad refers to global radiation, $[SO_2]$ to the concentration of sulfur dioxide and RH to relative humidity. CS is the condensation sink that we calculated from the particle size distributions measured with the DMPS assuming that the condensing vapor is sulfuric acid (Kulmala et al., 2001). Mikkonen et al. (2011) concluded that their proxy is suitable for estimating sulfuric acid concentration in a wide range of environmental conditions. Still, as there were no measurements of sulfuric acid concentration during our measurement campaign, the accuracy of the proxy in these specific conditions could not be assessed.

ACPD
15, 33077–33119, 2015

2.5 Trajectory analysis

To investigate the origin of air masses during the measurement campaign, we calculated 24 h backward trajectories using the HYSPLIT (Hybrid Single-Particle Lagrangian Integrated Trajectory) model (Draxler and Rolph, 2015). Global FNL meteorological archive generated by the NCEP GDAS (National Centers for Environmental Prediction Global Data Assimilation System) were used in the calculations. For each day we studied trajectories arriving at the measurement site hourly between 10 a.m. and 2 p.m. local winter time (UTC + 1 h) with the arrival height of 100 m. We determined the arrival direction of the air mass by dividing the trajectories into 22.5° sectors. If a trajectory spent over 70 % of the last 24 h before arriving to San Pietro Capofiume in a certain sector, that sector was selected to correspond to the arrival direction of the air mass.

3 Results and discussion

3.1 Meteorological conditions in San Pietro Capofiume during the PEGASOS campaign

The weather conditions during the campaign were initially characterized by moderate instability (from 8 to 14 June), which was followed by a series of sunny, hot days with relative humidity (RH) decreasing from day to day. The mean temperature for the campaign (25.5 °C) was 3.5 °C higher respect to a 15 year climatology for the site (data from the Regional Agency for Environmental Protection, ARPA, of Emilia-Romagna). The average RH was 16 % lower than typically, and the cumulated rain (24 mm) was half of the expected amount. In summary, the ambient conditions during the experiment were more representative for a heat-wave period than for an average summer in the Po Valley.

The meteorological conditions prevailing during the campaign resulted in the strong diurnal variation of radiation, temperature and RH. The median diurnal cycles of these variables are presented in Fig. 1 for new particle formation (NPF) event days (86 % of the days, see Sect. 3.3) and the only non-event day (6 July 2012) in local winter time (UTC + 1 h). On NPF event days global radiation started typically increase around 4 a.m. in the morning, and reached its maximum (940 W m^{-2}) at noon. Temperature began to increase from its nighttime values (about 20 °C) at the same time with the radiation and was highest (33 °C) around 3 p.m. The diurnal cycle of RH was opposite to that of temperature: RH was highest (84 %) early in the morning and lowest (30 %) in the afternoon. On the non-event day global radiation started to rise in the morning similarly as on event days but after reaching its maximum (820 W m^{-2}) around noon the radiation level dropped rapidly. Correspondingly, temperature also decreased in the afternoon being at that time 6–8 °C lower than typically on NPF event days. Furthermore, RH was higher on the non-event day than on event days exceeding 60 % in the afternoon. The results support previous studies from San Pietro Capofiume where NPF events have been observed to occur on days with high solar radiation and low RH (Hamed et al., 2007; Sogacheva et al., 2007).

Figure 1 also presents the median diurnal variation of PBL height. On NPF event days the progressive increase of the mixing layer from about 250 to 1700 m can be observed between 7 a.m. and 3 p.m. Therefore, the first steps of the photochemical processes observed at the station were triggered by reactions occurring in a rather thin atmospheric surface layer. Conversely, in the late morning and in the afternoon hours, the thickness of the PBL was great enough to allow the entrainment of air masses with their burden of chemical compounds travelling over long distances. On the non-event day the PBL height increased higher than typically on event days reaching about 2000 m. However, in the afternoon the PBL height quickly decreased being at that time about 1000 m lower than the PBL height typically on event days. Further analysis of ceilometer data reveals that low-level clouds were present in the morning and rainfall occurred between 2 and 3 p.m. on the non-event day, which explains the observed behaviour of radiation, RH and the PBL height. In agreement with our results, Sogacheva

ACPD
15, 33077–33119, 2015

et al. (2007) reported stronger mixing of PBL along the trajectories arriving to San Pietro Capofiume on NPF event days than on non-event days.

The effect of PBL height on background aerosol concentrations can be seen in the median diurnal variation of condensation sink (Fig. 1). Condensation sink was highest around 2 a.m. when boundary layer was still thin. The maximum value of condensation sink was higher on the non-event day ($0.023\,s^{-1}$) than typically on NPF event days ($0.015\,s^{-1}$). During the early morning, when the PBL started to form, condensation sink rapidly decreased and around 9 a.m. reached its daytime level (about $0.01\,s^{-1}$ both on NPF event days and on the non-event day). During the day, when mixing layer extended higher in the atmosphere, condensation sink stayed low starting to increase again after 6 p.m. Our observation on the lower condensation sink in the mornings of NPF event days compared to the non-event day is consistent with Hamed et al. (2007), who showed that low condensation sink favor particle formation in San Pietro Capofiume.

3.2 Concentrations of sub-3 nm clusters

A high number of sub-3 nm clusters was observed in San Pietro Capofiume during the measurement period (Fig. 2). The total concentration of 1.5–1.8 nm clusters varied from 610 to 11 930 cm^{-3} (5 and 95 % percentile) with the median concentration of 2140 cm^{-3}. The total concentration of 1.8–3.0 nm clusters varied from 2300 to 30 150 cm^{-3} (5 and 95 % percentile), while the median concentration was 7980 cm^{-3}. The majority of the observed sub-3 nm clusters were electrically neutral. The median concentrations of neutral clusters were 2090 and 7950 cm^{-3} in the size bins of 1.5–1.8 and 1.8–3 nm, respectively. The median positive ion concentrations were 20 and 4 cm^{-3} in the same size bins, and the median negative ion concentration was 6 cm^{-3} in both of the size bins. The concentrations of recombination products were also low: the median concentrations were 11 and 5 cm^{-3} in the size bins of 1.5–1.8 and 1.8–3 nm. The observed higher concentration of positive ions compared to negative ions may, at least partly, be due to the electrode effect, causing the accumulation of positive ions close to the Earth's surface (Hoppel et al., 1967).

ACPD
15, 33077–33119, 2015

Our results are in agreement with the earlier measurements from boreal forest in Finland, where a continuous population of sub-3 nm neutral clusters has been observed (Lehtipalo et al., 2009; Kulmala et al., 2013). However, the clusters concentrations observed in San Pietro Capofiume are about five times higher than the concentrations in the same size range in boreal forest. The observed cluster concentrations also exceed the concentrations of sub-3 nm clusters reported from a high-altitude site in France (Rose et al., 2015) and from two urban sites in the United States (Yu et al., 2014). On the other hand, at polluted sites in China, the sub-3 nm cluster concentrations were observed to be of the same order of magnitude as in San Pietro Capofiume (Xiao et al., 2015; Yu et al., 2015). This indicates that the formation of sub-3 nm clusters may be favored in areas where anthropogenic emissions of precursor vapors are high. Furthermore, our results support the earlier observations from boreal forest, where the contribution of ion-ion recombination to atmospheric cluster formation has been shown to be minor (Lehtipalo et al., 2009; Kontkanen et al., 2013).

3.3 New particle formation

NPF events were frequently observed during the measurement campaign (see Fig. 3). During the measurement period 86 % (19/22) of the days, from which we had NAIS data, were classified as NPF event days, while only one day was classified as a clear non-event case. On average, NPF is detected at the site less frequently, on 40–45 % of the days in June and on 65–70 % of days in July (Hamed et al., 2007; Manninen et al., 2010). High frequency of NPF events during our measurement campaign was likely related to favorable meteorological conditions with high solar radiation and low RH (see Sect. 3.1). Figure 4 shows the evolution of ion size distribution on a typical NPF event day (28 June) during the measurement campaign. The onset of NPF event can be observed around 7 a.m. and the growth of the ions can be followed until 5 p.m. in the evening.

The statistics of particle growth rates for the NPF events are shown in Table 1. The median growth rates in the size ranges of 1.5–3, 3–7 and 7–20 nm were 4.3, 6.0 and

ACPD
15, 33077–33119, 2015

$7.2\,\text{nm}\,\text{h}^{-1}$. Thus, the growth rate generally increased with the increasing particle size, which has been observed also at other measurement sites (Yli-Juuti et al., 2011; Kuang et al., 2012; Kulmala et al., 2013), and predicted by the so-called nano-Köhler theory describing the activation of nanometer-sized clusters by organic vapors (Kulmala et al., 2004b). By using BSMA (Balanced Scanning Mobility Analyzer) measurements, Manninen et al. (2010) obtained the median growth rate of $1.5\,\text{nm}\,\text{h}^{-1}$ for 1.5–3 nm particles in San Pietro Capofiume. The lower value of median growth rate compared to our results may be caused by their longer measurement period extending from March to October.

Table 2 presents the statistics of particle formation rates at 1.6 and at 2 nm during NPF events. The median formation rate of 1.6 nm clusters, $45\,\text{cm}^{-3}\,\text{s}^{-1}$, was one order of magnitude higher than the median formation rate of 2 nm clusters, $6.8\,\text{cm}^{-3}\,\text{s}^{-1}$. In earlier field measurements in boreal forest, Finland, the median particle formation rates were $5.9\,\text{cm}^{-3}\,\text{s}^{-1}$ at 1.5 nm and $1.9\,\text{cm}^{-3}\,\text{s}^{-1}$ at 2 nm (Kulmala et al., 2013). On the other hand, at a polluted site in Shanghai, China, the average formation rate of 1.3 nm clusters was observed to be $188\,\text{cm}^{-3}\,\text{s}^{-1}$ (Xiao et al., 2015). Thus, it seems that the formation rates of sub-3 nm clusters are in San Pietro Capofiume higher than in clean boreal forest environment but still lower than at a polluted urban site. This indicates that high background aerosol concentrations do not necessarily inhibit the formation of sub-3 nm clusters if the concentrations of precursor vapors are high enough. The median condensation sink in San Pietro Capofiume was $1.1 \times 10^{-2}\,\text{s}^{-1}$ during the measurement period. In boreal forest, Finland, typical condensation sink on NPF event days has been observed to be about $2 \times 10^{-3}\,\text{s}^{-1}$ (Dal Maso et al., 2005; Kulmala et al., 2013), and in Shanghai, China, $6 \times 10^{-2}\,\text{s}^{-1}$ (Xiao et al., 2015).

The median formation rates of 1.6 nm positive and negative ions (0.19 and $0.06\,\text{cm}^{-3}\,\text{s}^{-1}$) were two orders of magnitude lower than the formation rate of 1.6 nm total clusters (Table 2). In addition, the median formation rates of 2 nm positive ions ($0.12\,\text{cm}^{-3}\,\text{s}^{-1}$) and negative ions ($0.08\,\text{cm}^{-3}\,\text{s}^{-1}$) were one order of magnitude lower than the formation rate of 2 nm total clusters. Thus, neutral pathways seem to domi-

ACPD
15, 33077–33119, 2015

nate particle formation in San Pietro Capofiume. These results are consistent with the earlier observations from boreal forest in Finland and at a high-altitude site in France, where the formation rate of 1.5 nm total clusters has been found to clearly exceed the formation rate of 1.5 nm ions (Kulmala et al., 2013; Rose et al., 2015). Manninen et al. (2010) reported slightly lower values for the median formation rates of 2 nm ions (0.06 $cm^{-3} s^{-1}$ for both polarities) based on their BSMA measurements in San Pietro Capofiume but, as mentioned above, their measurement period was longer than ours.

To further investigate the contribution of ions to particle formation, we calculated the ion-induced nucleation fraction for each NPF event by dividing the ion formation rate by the total formation rate. The median ion-induced nucleation fraction was 0.7 % at 1.6 nm and 3.0 % at 2 nm. This further demonstrates that ions have only a minor contribution to the formation of sub-3 nm clusters in San Pietro Capofiume. The higher ion-induced nucleation fraction at 2 nm than at 1.6 nm suggests that ions at 2 nm may be formed by coagulation between small ions and neutral clusters. In previous studies the ion-induced nucleation fraction has been observed to be typically low, less than 10 %, in the continental boundary layer (Iida et al., 2006; Manninen et al., 2010).

3.4 Diurnal variation of cluster concentrations and formation rates

Figure 5 shows the median diurnal variation of the concentrations of neutral clusters, charged clusters and recombination products on NPF event days and on the only non-event day. In addition, the variation of PBL height is presented. The concentrations of neutral 1.5–1.8 nm and 1.8–3.0 nm clusters were high throughout the day on NPF event days and on the non-event day. On NPF event days the neutral cluster concentrations had maxima around 9 a.m., which could not be observed on the non-event day. The neutral cluster concentration in the size bin of 1.5–1.8 nm reached the maximum earlier than the concentration in the larger, 1.8–3 nm, size bin. The daytime maximum on NPF event days can also be detected in the concentrations of ions and recombination product in the size bin of 1.8–3.0 nm. Nevertheless, the peak ion concentrations were about three orders of magnitude lower than those of neutral clusters. In the smaller size

ACPD
15, 33077–33119, 2015

bin (1.5–1.8 nm) these maxima were not as clear. The reason for this is that small ions are continuously formed in the atmosphere as a result of ionization of air molecules, while larger ions are usually present only during NPF events (e.g. Hirsikko et al., 2011). The observed diurnal cycle of the cluster concentrations is generally similar as in the earlier observations made in boreal forest, Finland (Kulmala et al., 2013), and at urban sites in the United States and China (Yu et al., 2014, 2015; Xiao et al., 2015).

To study the contribution of ions to cluster concentrations, we also examined the diurnal variation of the fraction of ions of all clusters on NPF event days (Fig. 6). The ion fraction in the size bin of 1.5–1.8 nm varied between 0.3 and 2 %. The lowest values were obtained slightly after 9 a.m., which is due to the strong increase in the neutral cluster concentration during NPF event (Fig. 5). In the size bin of 1.8–3 nm, the ion fraction was most of the time very low (about 0.2 %), but peaked before 9 a.m. reaching 0.5 %. This is likely caused by the fact that the concentration of ions in the size bin of 1.8–3 nm started to increase earlier on NPF event days than the concentration of neutral clusters in the same size bin (Fig. 5). Similar observations have been earlier reported by Gonser et al. (2014).

In Fig. 7 the median diurnal variation of particle formation rates are presented together with the PBL height for NPF event days and for the only non-event day. The formation rate of 1.6 nm total clusters varied between 8 and 68 $cm^{-3}\,s^{-1}$ on NPF event days, reaching the highest values around 9 a.m. On the non-event day the formation rate was lower, varying between 2 and 14 $cm^{-3}\,s^{-1}$. Similarly, the formation rate of 2 nm clusters had a maximum of 7 $cm^{-3}\,s^{-1}$ on NPF event days, and on the non-event day it varied between 0.1 and 3 $cm^{-3}\,s^{-1}$. The formation rates of ions were at both sizes clearly lower than the total formation rates. The maximum formation rate of 1.6 nm ions on NPF event days was 0.19 $cm^{-3}\,s^{-1}$ for positive ions and 0.09 $cm^{-3}\,s^{-1}$ for negative ions. At 2 nm, the corresponding maximum formation rate was 0.13 $cm^{-3}\,s^{-1}$ for positive ions and 0.11 $cm^{-3}\,s^{-1}$ for negative ions. On the non-event day the ion formation rates were even lower than on event days. Overall, these results suggest that sub-3 nm clusters are formed continuously, also outside NPF events. Furthermore, as concluded

ACPD
15, 33077–33119, 2015

already above, neutral nucleation mechanisms seem to dominate in San Pietro Capofiume. Our results support earlier observations obtained in field measurement in boreal forest by Kulmala et al. (2013).

When comparing the diurnal variations of cluster concentrations and their formation rates with the diurnal cycle of PBL height and other meteorological parameters, similarities can be found. At the same time as the concentrations and formation rates of clusters started to increase in the morning of NPF event days, after 7 a.m., the PBL height also started to increase. Furthermore, at this time radiation and temperature had already started to rise from their low nigh-times values and, reversely, RH and condensation sink were decreasing (Fig. 1). This indicates that the sunrise can be important for the formation of atmospheric clusters due to several processes. Firstly, the build-up of PBL, induced by the heating of solar radiation, dilutes the background aerosol concentration and thus reduces the condensation sink. On the other hand, solar radiation also triggers the photochemical production of precursor vapors, which may form clusters due to their low volatility. Finally, increasing temperature also lowers RH. On the other hand, it needs to be noted that the formation of sub-2 nm clusters was observed to take place continuously, also at night (see Fig. 7). Thus, the formation of the smallest clusters seems to occur also without solar radiation, which indicates that they may be formed, for example, by the low-volatility vapors produced in the ozonolysis of organic vapors (Ehn et al., 2014; Jokinen et al., 2014).

3.5 Effect of sulfuric acid concentration and condensation sink on cluster concentrations

San Pietro Capofiume is located in the industrialized Po Valley with many emission sources for anthropogenic pollutants. According to Sogacheva et al. (2007), more than 40 % of SO_2 emissions over the Po Valley can be observed at the San Pietro Capofiume station. SO_2 is a precursor for sulfuric acid that is known to be a key compound in atmospheric cluster formation (e.g. Weber et al., 1997; Sipilä et al., 2010; Kirkby et al., 2011). Hamed et al. (2007) concluded that in San Pietro Capofiume daytime

ACPD
15, 33077–33119, 2015

Title Page
Abstract | Introduction
Conclusions | References
Tables | Figures
◂◂ | ▸▸
◂ | ▸
Back | Close
Full Screen / Esc
Printer-friendly Version
Interactive Discussion

SO_2 concentrations are clearly higher on NPF event days than on non-event days in summertime. To investigate the importance of sulfuric acid for cluster formation in San Pietro Capofiume, we studied the correlation between the concentrations of neutral and charged clusters and sulfuric acid proxy. Furthermore, to see how the concentrations of large background aerosol particles affect cluster concentrations, the correlation between cluster concentrations and condensation sink was examined.

In agreement with earlier studies, the sub-3 nm cluster concentrations correlated positively with sulfuric acid proxy indicating that sulfuric acid is essential for cluster formation in San Pietro Capofiume (Fig. 8). For neutral clusters the positive correlation was evident both in the size bin of 1.5–1.8 nm ($R = 0.60$) and in the size bin of 1.8–3 nm ($R = 0.68$). Ions had a weaker correlation in the size bin of 1.5–1.8 nm ($R = 0.48$) than in the size bin of 1.8–3 nm ($R = 0.68$). This is expected, as the small ions are produced continuously due to ionization of air molecules, whereas larger ions are formed during NPF events by, for example, the charging of small neutral clusters. Our result is consistent with the previous studies where sub-3 nm clusters have been observed to be associated with high sulfuric acid concentrations (Kulmala et al., 2013; Yu et al., 2014).

The relation between the sub-3 nm cluster concentrations and condensation sink is presented in Fig. 9. It seems that the concentration of neutral clusters does not have a negative correlation with condensation sink as one would expect. This indicates that in San Pietro Capofiume the formation of neutral clusters may, at least partly, be linked to anthropogenic emissions with high concentrations of low-volatile precursor vapors but also high condensation sink. Furthermore, ions had a negative correlation with the condensation sink especially in the size bin of 1.5–1.8 nm ($R = -0.59$). In the size bin of 1.8–3 nm the negative correlation was weaker ($R = -0.37$).

3.6 Effect of air mass origin

By using back-trajectory analysis, we investigated how the air mass origin affects the sub-3 nm cluster concentrations, and their precursors and sinks in San Pietro Capofiume. Figure 10 illustrates the air mass arrival directions and their relation to the total

ACPD
15, 33077–33119, 2015

concentration of 1.8–3.0 nm clusters, sulfuric acid proxy, and condensation sink in San Pietro Capofiume around midday (between 10 a.m. and 2 p.m.). A clear majority of air masses arrived to San Pietro Capofiume from northeastern to eastern directions and from the southwest during the measurement campaign. When air masses were coming from northeastern to eastern directions the sub-3 nm cluster concentrations were most of the time high (> 3×10^4 cm^{-3}). When air masses originated from the southwest, lower concentrations were more frequent. Moreover, the southwestern direction was often related to high condensation sink (> 1.2×10^{-2} s^{-1}). On the other hand, high values of condensation sink were observed also when air masses were coming from the northeast. For sulfuric acid proxy, there was no clear difference between the northeastern and southwestern directions, but high concentrations (> 2.4×10^7 cm^{-3}) were linked to both of these directions.

All in all, it seems that the northeastern direction was more favorable for the formation of sub-3 nm clusters than the southwestern direction during our measurement campaign. In previous studies air masses related to particle formation have also been observed to arrive to San Pietro Capofiume mostly from eastern directions (Hamed et al., 2007; Sogacheva et al., 2007). Furthermore, Hamed et al. (2007) reported that in all seasons except summer, the eastern directions were associated with the lower value of condensation sink than the western directions. In summer, they did not observe a clear difference in condensation sink between eastern and western air masses. This is in agreement with our results which do not show significantly lower condensation sink related to the northwestern direction than the southwestern direction. Thus, it seems that during our measurement campaign the precursor vapors of the clusters and large background aerosol particles, which act as a sink for clusters, may have originated from the same sources. This is consistent with the fact that no negative correlation was found between neutral sub-3 nm clusters and condensation sink, as discussed in Sect. 3.5. The possible sources of background aerosol particles and precursor vapors include anthropogenic emissions from power plants and industrial areas in the Po Valley, ship traffic in the Adriatic Sea, and long-range transport from Central and Eastern Europe (Hamed et al., 2007; Sogacheva et al., 2007).

4 Conclusions

A high concentration of sub-3 nm clusters was observed in San Pietro Capofiume measurement site during the PEGASOS campaign (7 June–9 July 2012). The median cluster concentrations were 2140 and 7980 cm^{-3} in the size bins of 1.5–1.8 nm and 1.8–3 nm. The majority of clusters were electrically neutral; the median ion fraction was 1.2 % in the size bin of 1.5–1.8 nm and 0.1 % in the size bin of 1.8–3 nm. The observed sub-3 nm cluster concentrations were of the same order of magnitude as at polluted sites in China (Xiao et al., 2015; Yu et al., 2015), but higher than in clean boreal forest in Finland (Kulmala et al., 2013) and at urban sites in the United States (Yu et al., 2014).

New particle formation (NPF) events were observed during the measurement period very frequently, on 86 % of the days. The median growth rates of clusters during the events were 4.3, 6.0 and 7.2 $nm\,h^{-1}$ in the size ranges of 1.5–3 nm, 3–7 nm and 7–20 nm. Thus, the growth rate increased with size, which has been observed also at other measurement sites (e.g. Yli-Juuti et al., 2011) and predicted by the so-called nano-Köhler theory (Kulmala et al., 2004b). The median formation rate of 1.6 nm clusters was 45 $cm^{-3}\,s^{-1}$, exceeding the median formation rate of 2 nm clusters by one order of magnitude. The observed formation rates were higher than in clean boreal forest environment but lower than at a highly polluted urban site (Kulmala et al., 2013; Xiao et al., 2014). Furthermore, the median formation rates of ions were clearly lower than the formation rates of total clusters at all sizes. The median ion-induced nucleation fraction was 0.7 % at 1.6 nm and 3.0 % at 2 nm. This indicates that neutral pathways dominate the sub-3 nm cluster formation in San Pietro Capofiume, similarly as in boreal forest (Kulmala et al., 2013). The median condensation sink during the measurement

ACPD
15, 33077–33119, 2015

period was relatively high ($1.1 \times 10^{-2}\,s^{-1}$), which demonstrates that high background aerosol concentrations do not necessarily inhibit the formation of sub-3 nm clusters.

When studying the diurnal variation of cluster concentrations, we observed that the concentrations of neutral 1.5–1.8 nm and 1.8–3.0 nm clusters were high both on NPF event and non-event days. However, on NPF event days cluster concentrations had maxima around 9 a.m. which were absent on non-event days. Similarly, ion concentrations in the size bin of 1.8–3 nm peaked on NPF event days, reaching the maximum slightly earlier than neutral clusters. The formation rates of clusters had also maxima around 9 a.m. on NPF event days. Still, the formation of sub-3 nm clusters was observed to take place continuously, also outside NPF events. Moreover, the increase in the concentrations and formation rates of clusters in the morning took place simultaneously with the build-up of planetary boundary layer (PBL). In addition, radiation and temperature were rising and RH and condensation sink declining at that time. Thus, the changes in the local meteorological conditions triggered by the sunrise in the morning may be important drivers of cluster formation at the San Pietro Capofiume station.

Finally, we also studied the correlation of the sub-3 nm cluster concentrations with sulfuric acid proxy and condensation sink. Sulfuric acid proxy had a positive correlation with the neutral cluster concentrations. This indicates that sulfuric acid has an important role in the formation of sub-3 nm clusters in San Pietro Capofiume, as has been observed also at other measurement sites (Kulmala et al., 2013; Yu et al., 2014). The concentration of charged clusters had a negative correlation with condensation sink, but we did not found any relation between the neutral cluster concentrations and condensation sink. By using back-trajectory analysis, we observed that the sub-3 nm cluster concentrations were typically higher when air masses arrived to San Pietro Capofiume from northeastern directions than from the southwest. On the other hand, it seems that precursor vapors of clusters and background aerosol particles, acting as their sink, may have originated from the same sources. The potential sources include anthropogenic emissions from power plants and industrial areas in the Po Valley, maritime traffic in the Adriatic Sea, and long-range transport from Central and Eastern Europe (Hamed et al., 2007; Sogacheva et al., 2007).

Acknowledgements. This research was supported by the European Commission under the Framework Programme 7 (PEGASOS project, FP7-ENV-2010-265148), the European Research Council (ERC) Advanced Grant (ATM-NUCLE, 227463), and the European Union's Horizon 2020 research and innovation programme under the Marie Sklodowska-Curie grant agreement No. 656994. The support by the Academy of Finland Centre of Excellence program (project no. 1118615 and 272041) is also gratefully acknowledged.

References

Aalto, P., Hämeri, K., Becker, E.,Weber, R., Salm, J., Mäkelä, J. M., Hoell, C., O'Dowd, C. D., Karlsson, H., Hansson, H.-C., Väkevä, M., Koponen, I. K., Buzorius, G., and Kulmala, M.: Physical characterization of aerosol particles during nucleation events, Tellus, 53 B, 344–358, 2001.

Almeida, J., Schobesberger, S., Kurten, A., Ortega, I., Kupiainen-Määtta, O., Praplan, A., Adamov, A., Amorim, A., Bianchi, F., Breitenlechner, M., David, A., Dommen, J., Donahue, N., Downard, A., Dunne, E., Duplissy, J., Ehrhart, S., Flagan, R., Franchin, A., Guida, R., Hakala, J., Hansel, A., Heinritzi, M., Henschel, H., Jokinen, T., Junninen, H., Kajos, M., Kangasluoma, J., Keskinen, H., Kupc, A., Kurten, T., Kvashin, A., Laaksonen, A., Lehtipalo, K., Leiminger, M., Leppä, J., Loukonen, V., Makhmutov, V., Mathot, S., McGrath, M., Nieminen, T., Olenius, T., Onnela, A., Petaja, T., Riccobono, F., Riipinen, I., Rissanen, M., Rondo, L., Ruuskanen, T., Santos, F., Sarnela, N., Schallhart, S., Schnitzhofer, R., Seinfeld, J., Simon, M., Sipila, M., Stozhkov, Y., Stratmann, F., Tome, A., Trostl, J., Tsagkogeorgas, G., Vaattovaara, P., Viisanen, Y., Virtanen, A., Vrtala, A., Wagner, P., Weingartner, E., Wex, H., Williamson, C., Wimmer, D., Ye, P., Yli-Juuti, T., Carslaw, K., Kulmala, M., Curtius, J., Baltensperger, U., Worsnop, D., Vehkamäki, H., and Kirkby, J.: Molecular understanding of sulphuric acid-amine particle nucleation in the atmosphere, Nature, 502, 359–363, doi:10.1038/nature12663, 2013.

Angelini, A. and Gobbi, G. P.: Some remarks about lidar data preprocessing and different implementations of the gradient method for determining the aerosol layers, Ann. Geophys. Italy, 57, A0218, doi:10.4401/ag-6408, 2014.

Boy, M. and Kulmala, M.: Nucleation events in the continental boundary layer: Influence of physical and meteorological parameters, Atmos. Chem. Phys., 2, 1–16, doi:10.5194/acp-2-1-2002, 2002.
Dal Maso, M., Kulmala, M., Riipinen, I., Wagner, R., Hussein, T., Aalto, P. P., and Lehtinen, K. E. J.: Formation and growth of fresh atmospheric aerosols: eight years of aerosol size distribution data from SMEAR II, Hyytiälä, Finland, Boreal Environ. Res., 10, 323–336, 2005.
Di Giuseppe, F., Riccio, A., Caporaso, L., Bonafè, G., Gobbi, G. P., and Angelini, F.: Automatic detection of atmospheric boundary layer height using ceilometer backscatter data assisted by a boundary layer model, Q. J. Roy. Meteor. Soc., 138, 649–663, doi:10.1002/qj.964, 2012.
Draxler, R. R. and Rolph, G. D.: HYSPLIT (HYbrid Single-Particle Lagrangian Integrated Trajectory), model access via NOAA ARL READY Website, NOAA Air Resources Laboratory, Silver Spring, MD, available at: http://www.arl.noaa.gov/ready/hysplit4.html, last access: 13 January 2015.
Ehn, M., Thornton, J. A., Kleist, E., Sipilä, M., Junninen, H., Pullinen, I., Springer, M., Rubach, F., Tillmann, R., Lee, B., Lopez-Hilfiker, F., Andres, S., Acir, I.-H., Rissanen, M., Jokinen, T., Schobesberger, S., Kangasluoma, J., Kontkanen, J., Nieminen, T., Kurtén, T., Nielsen, L. B., Jørgensen, S., Kjaergaard, H. G., Canagaratna, M., Dal Maso, M., Berndt, T., Petäjä, T., Wahner, A., Kerminen, V., Kulmala, M., Worsnop, D. R., Wildt, J., and Mentel, T. F.: A large source of low-volatility secondary organic aerosol, Nature, 506, 476–479, doi:10.1038/nature13032, 2014.
Gonser, S. G., Klein, F., Birmili, W., Größ, J., Kulmala, M., Manninen, H. E., Wiedensohler, A., and Held, A.: Ion – particle interactions during particle formation and growth at a coniferous forest site in central Europe, Atmos. Chem. Phys., 14, 10547–10563, doi:10.5194/acp-14-10547-2014, 2014.
Günther, A. B., Jiang, X., Heald, C. L., Sakulyanontvittaya, T., Duhl, T., Emmons, L. K., and Wang, X.: The Model of Emissions of Gases and Aerosols from Nature version 2.1 (MEGAN2.1): an extended and updated framework for modeling biogenic emissions, Geosci. Model Dev., 5, 1471–1492, doi:10.5194/gmd-5-1471-2012, 2012.
Hamed, A., Joutsensaari, J., Mikkonen, S., Sogacheva, L., Dal Maso, M., Kulmala, M., Cavalli, F., Fuzzi, S., Facchini, M. C., Decesari, S., Mircea, M., Lehtinen, K. E. J., and Laaksonen, A.: Nucleation and growth of new particles in Po Valley, Italy, Atmos. Chem. Phys., 7, 355–376, doi:10.5194/acp-7-355-2007, 2007.

ACPD
15, 33077–33119, 2015

High concentrations of sub-3 nm clusters and frequent new particle formation

J. Kontkanen et al.

Hamed, A., Korhonen, H., Sihto, S.-L., Joutsensaari, J., Järvinen, H., Petäjä, T., Arnold, F., Nieminen, T., Kulmala, M., Smith, J. N., Lehtinen, K. E. J., and Laaksonen, A.: The role of relative humidity in continental new particle formation, J. Geophys. Res., 116, D03202, doi:10.1029/2010JD014186, 2011.
Hirsikko, A., Laakso, L., Hõrrak, U., Aalto, P. P., Kerminen, V.-M., and Kulmala, M.: Annual and size dependent variation of growth rates and ion concentrations in boreal forest, Boreal Environ. Res., 10, 357–369, 2005.
Hirsikko, A., Bergman, T., Laakso, L., Dal Maso, M., Riipinen, I., Hõrrak, U., and Kulmala, M.: Identification and classification of the formation of intermediate ions measured in boreal forest, Atmos. Chem. Phys., 7, 201–210, doi:10.5194/acp-7-201-2007, 2007.
Hirsikko, A., Nieminen, T., Gagné, S., Lehtipalo, K., Manninen, H. E., Ehn, M., Hõrrak, U., Kerminen, V.-M., Laakso, L., McMurry, P. H., Mirme, A., Mirme, S., Petäjä, T., Tammet, H., Vakkari, V., Vana, M., and Kulmala, M.: Atmospheric ions and nucleation: a review of observations, Atmos. Chem. Phys., 11, 767–798, doi:10.5194/acp-11-767-2011, 2011.
Hoppel, W. A.: Theory of the electrode effect, J. Atmos. Terr. Phys., 29, 709–721, 1967.
Hoppel, W. A. and Frick, G. M.: Ion-aerosol attachment coefficients and the steady-state charge distribution on aerosols in a bipolar ion environment, Aerosol Sci. Tech., 5, 1–21, 1986.
Hyvönen, S., Junninen, H., Laakso, L., Dal Maso, M., Grönholm, T., Bonn, B., Keronen, P., Aalto, P., Hiltunen, V., Pohja, T., Launiainen, S., Hari, P., Mannila, H., and Kulmala, M.: A look at aerosol formation using data mining techniques, Atmos. Chem. Phys., 5, 3345–3356, doi:10.5194/acp-5-3345-2005, 2005.
Iida, K., Stolzenburg, M., McMurry, P. H., Dunn, M. J., Smith, J. N., Eisele, F., and Keady, P.: Contribution of ion-induced nucleation to new particle formation: methodology and its application to atmospheric observations in Boulder, Colorado, J. Geophys. Res., 111, D23201, doi:10.1029/2006JD007167, 2006.
Jokinen, T., Sipilä, M., Richters, S., Kerminen, V.-M., Paasonen, P., Stratmann, F., Worsnop, D., Kulmala, M., Ehn, M., Herrmann, H., and Berndt, T.: Rapid autoxidation forms highly oxidized RO_2 radicals in the atmosphere, Angwe. Chem. Int. Edit., 53, 14596–14600, doi:10.1002/anie.201408566, 2014.
Kazil, J., Stier, P., Zhang, K., Quaas, J., Kinne, S., O'Donnell, D., Rast, S., Esch, M., Ferrachat, S., Lohmann, U., and Feichter, J.: Aerosol nucleation and its role for clouds and Earth's radiative forcing in the aerosol-climate model ECHAM5-HAM, Atmos. Chem. Phys., 10, 10733–10752, doi:10.5194/acp-10-10733-2010, 2010.

Kerminen, V.-M., Pirjola, L., and Kulmala, M.: How significantly does coagulational scavenging limit atmospheric particle production?, J. Geophys. Res., 125, 119–124, 2001.
Kirkby, J., Curtius, J., Almeida, J., Dunne, E., Duplissy, J., Ehrhart, S., Franchin, A., Gagné, S., Ickes, L., Kürten, A., Kupc, A., Metzger, A., Riccobono, F., Rondo, L., Schobesberger, S., Tsagkogeorgas, G., Wimmer, D., Amorim, A., Bianchi, F., Breitenlechner, M., David, A., Dommen, J., Downard, A., Ehn, M., Flagan, R. C., Haider, S., Hansel, A., Hauser, D., Jud, W., Junninen, H., Kreissl, F., Kvashin, A., Laaksonen, A., Lehtipalo, K., Lima, J., Lovejoy, E. R., Makhutov, V., Mathot, S., Mikkilä, J., Minginette, P., Mogo, S., Nieminen, T., Onnela, A., Pereira, A., Petäjä, T., Schnitzhofer, R., Seinfeld, J. H., Sipilä, M., Stozhkov, Y., Stratmann, F., Tome, A., Vanhanen, J., Viisanen, Y., Vrtala, A., Wagner, P. E., Walther, H., Weingartner, E., Wex, H., Winkler, P. M., Carslaw, K. S., Worsnop, D. R., Baltensperger, U., and Kulmala, M.: The role of sulfuric acid, ammonia and galactic cosmic rays in atmospheric aerosol nucleation, Nature, 476, 429–433, 2011.
Kontkanen, J., Lehtinen, K. E. J., Nieminen, T., Manninen, H. E., Lehtipalo, K., Kerminen, V.-M., and Kulmala, M.: Estimating the contribution of ion–ion recombination to sub-2 nm cluster concentrations from atmospheric measurements, Atmos. Chem. Phys., 13, 11391–11401, doi:10.5194/acp-13-11391-2013, 2013.
Korhonen, H., Sihto, S.-L., Kerminen, V.-M., and Lehtinen, K. E. J.: Evaluation of the accuracy of analysis tools for atmospheric new particle formation, Atmos. Chem. Phys., 11, 3051–3066, doi:10.5194/acp-11-3051-2011, 2011.
Kuang, C., Chen, M., Zhao, J., Smith, J., McMurry, P. H., and Wang, J.: Size and time-resolved growth rate measurements of 1 to 5 nm freshly formed atmospheric nuclei, Atmos. Chem. Phys., 12, 3573–3589, doi:10.5194/acp-12-3573-2012, 2012.
Kulmala, M., Toivonen, A., Mäkelä, J. M., and Laaksonen, A.: Analysis of the growth of nucleation mode particles observed in Boreal forest, Tellus B, 50, 449–462, 1998.
Kulmala, M., Maso, M. D., Mäkelä, J. M., Pirjola, L., Väkevä, M., Aalto, P., Miikkulainen, P., Hämeri, K., and O'Dowd, C. D.: On the formation, growth and composition of nucleation mode particles, Tellus B, 53, 479–490, 2001.
Kulmala, M., Vehkamäki, H., Petäjä, T., Dal Maso, M., Lauri, A., Kerminen, V.-M., Birmili, W., and McMurry, P. H.: Formation and growth rates of ultrafine atmospheric particles: A review of observations, J. Aerosol Sci., 35, 143–176, 2004a.

ACPD
15, 33077–33119, 2015

High concentrations of sub-3 nm clusters and frequent new particle formation

J. Kontkanen et al.

Kulmala, M., Kerminen, V.-M., Anttila, T., Laaksonen, A., and O'Dowd, C. D.: Organic aerosol formation via sulphate cluster activation, J. Geophys. Res., 109, 4205, doi:10.1029/2003JD003961, 2004b.

Kulmala, M., Riipinen, I., Sipila, M., Manninen, H. E., Petaja, T., Junninen, H., dal Maso, M., Mordas, G., Mirme, A., Vana, M., Hirsikko, A., Laasko, L., Harrison, R. M., Hanson, I., Leung, C., Lehtinen, K. E. J., and Kerminen, V.-M.: Toward direct measurement of atmospheric nucleation, Science, 318, 89–92, 2007.

Kulmala, M., Petäjä, T., Nieminen, T., Sipilä, M., Manninen, H. E., Lehtipalo, K., Dal Maso, M., Aalto, P. P., Junninen, H., Paasonen, P., Riipinen, I., Lehtinen, K. E. J., Laaksonen, A., and Kerminen, V.-M.: Measurement of the nucleation of atmospheric aerosol particles, Nat. Protoc., 7, 1651–1667, doi:10.1038/nprot.2012.091, 2012.

Kulmala, M., Kontkanen, J., Junninen, H., Lehtipalo, K., Manninen, H. E., Nieminen, T., Petäjä, T., Sipilä, M., Schobesberger, S., Rantala, P., Franchin, A., Jokinen, T., Järvinen, E., Äijälä, M., Kangasluoma, J., Hakala, J., Aalto, P. P., Paasonen, P., Mikkilä, J., Vanhanen, J., Aalto, J., Hakola, H., Makkonen, U., Ruuskanen, T., Mauldin, R. L., Duplissy, J., Vehkamäki, H., Bäck, J., Kortelainen, A., Riipinen, I., Kurtén, T., Johnston, M. V, Smith, J. N., Ehn, M., Mentel, T. F., Lehtinen, K. E. J., Laaksonen, A., Kerminen, V.-M., and Worsnop, D. R.: Direct observations of atmospheric aerosol nucleation, Science, 339, 943–946, doi:10.1126/science.1227385, 2013.

Kulmala, M., Petäjä, T., Ehn, M., Thornton, J., Sipilä, M., Worsnop, D. R., and Kerminen, V.-M.: Chemistry of atmospheric nucleation: on the recent advances on precursor characterization and atmospheric cluster composition in connection with atmospheric new particle formation, Annu. Rev. Phys. Chem., 65, 21–37, 2014.

Laaksonen, A., Hamed, A., Joutsensaari, J., Hiltunen, L., Cavalli, F., Junkermann, W., Asmi, A., Fuzzi, S., and Facchini, M. C.: Cloud condensation nucleus production from nucleation events at a highly polluted region, Geophys. Res. Lett., 32, L06812, doi:10.1029/2004GL022092, 2005.

Lehtipalo, K., Sipilä, M., Riipinen, I., Nieminen, T., and Kulmala, M.: Analysis of atmospheric neutral and charged molecular clusters in boreal forest using pulse-height CPC, Atmos. Chem. Phys., 9, 4177–4184, doi:10.5194/acp-9-4177-2009, 2009.

Lehtipalo, K., Kulmala, M., Sipilä, M., Petäjä, T., Vana, M., Ceburnis, D., Dupuy, R., and O'Dowd, C.: Nanoparticles in boreal forest and coastal environment: a comparison of obser-

vations and implications of the nucleation mechanism, Atmos. Chem. Phys., 10, 7009–7016, doi:10.5194/acp-10-7009-2010, 2010.
Makkonen, R., Asmi, A., Kerminen, V.-M., Boy, M., Arneth, A., Hari, P., and Kulmala, M.: Air pollution control and decreasing new particle formation lead to strong climate warming, Atmos. Chem. Phys., 12, 1515–1524, doi:10.5194/acp-12-1515-2012, 2012.
Manninen, H. E., Nieminen, T., Asmi, E., Gagné, S., Häkkinen, S., Lehtipalo, K., Aalto, P., Vana, M., Mirme, A., Mirme, S., Hõrrak, U., Plass-Dülmer, C., Stange, G., Kiss, G., Hoffer, A., Törő, N., Moerman, M., Henzing, B., de Leeuw, G., Brinkenberg, M., Kouvarakis, G. N., Bougiatioti, A., Mihalopoulos, N., O'Dowd, C., Ceburnis, D., Arneth, A., Svenningsson, B., Swietlicki, E., Tarozzi, L., Decesari, S., Facchini, M. C., Birmili, W., Sonntag, A., Wiedensohler, A., Boulon, J., Sellegri, K., Laj, P., Gysel, M., Bukowiecki, N., Weingartner, E., Wehrle, G., Laaksonen, A., Hamed, A., Joutsensaari, J., Petäjä, T., Kerminen, V.-M., and Kulmala, M.: EUCAARI ion spectrometer measurements at 12 European sites – analysis of new particle formation events, Atmos. Chem. Phys., 10, 7907–7927, doi:10.5194/acp-10-7907-2010, 2010.
Merikanto, J., Spracklen, D. V., Mann, G. W., Pickering, S. J., and Carslaw, K. S.: Impact of nucleation on global CCN, Atmos. Chem. Phys., 9, 8601–8616, doi:10.5194/acp-9-8601-2009, 2009.
Metzger, A., Verheggen, B., Dommen, J., Duplissy, J., Prevot, A. S., Weingartner, E., Riipinen, I., Kulmala, M., Spracklen, D. V., Carslaw, K. S., and Baltensperger, U.: Evidence for the role of organics in aerosol particle formation under atmospheric conditions, P. Natl. Acad. Sci. USA, 107, 6646–6651, doi:10.1073/pnas.0911330107, 2010.
Mikkonen, S., Romakkaniemi, S., Smith, J. N., Korhonen, H., Petäjä, T., Plass-Duelmer, C., Boy, M., McMurry, P. H., Lehtinen, K. E. J., Joutsensaari, J., Hamed, A., Mauldin III, R. L., Birmili, W., Spindler, G., Arnold, F., Kulmala, M., and Laaksonen, A.: A statistical proxy for sulphuric acid concentration, Atmos. Chem. Phys., 11, 11319–11334, doi:10.5194/acp-11-11319-2011, 2011.
Mirme, S. and Mirme, A.: The mathematical principles and design of the NAIS – a spectrometer for the measurement of cluster ion and nanometer aerosol size distributions, Atmos. Meas. Tech., 6, 1061–1071, doi:10.5194/amt-6-1061-2013, 2013.
Mirme, S., Mirme, A., Minikin, A., Petzold, A., Hõrrak, U., Kerminen, V. -M., and Kulmala, M.: Atmospheric sub-3 nm particles at high altitudes, Atmos. Chem. Phys., 10, 437–451, doi:10.5194/acp-10-437-2010, 2010.

ACPD
15, 33077–33119, 2015

Nieminen, T., Yli-Juuti, T., Manninen, H. E., Petäjä, T., Kerminen, V.-M., and Kulmala, M.: Technical note: New particle formation event forecasts during PEGASOS-Zeppelin Northern mission 2013 in Hyytiälä, Finland, Atmos. Chem. Phys., 15, 12385–12396, doi:10.5194/acp-15-12385-2015, 2015.

Nilsson, E. D., Rannik, Ü., Kulmala, M., Buzorius, G., and O'Dowd, C.: Effects of the continental boundary layer evolution, convection, turbulence and entrainment on aerosol formation, Tellus B, 53, 441–461, 2001a.

Nilsson, E. D., Paatero, J., and Boy, M.: Effects of air masses and synoptic weather on aerosol formation in the continental boundary layer, Tellus B, 53, 462–478, 2001b.

Riccobono, F., Schobesberger, S., Scott, C. E., Dommen, J., Ortega, I. K., Rondo, L., Almeida, J., Amorim, A., Bianchi, F., Breitenlechner, M., David, A., Downard, A., Dunne, E. M., Duplissy, J., Ehrhart, S., Flagan, R. C., Franchin, A., Hansel, A., Junninen, H., Kajos, M., Keskinen, H., Kupc, A., Kürten, A., Kvashin, A. N., Laaksonen, A., Lehtipalo, K., Makhmutov, V., Mathot, S., Nieminen, T., Onnela, A., Petäjä, T., Praplan, A. P., Santos, F. D., Schallhart, S., Seinfeld, J. H., Sipilä, M., Spracklen, D. V., Stozhkov, Y., Stratmann, F., Tomé, A., Tsagkogeorgas, G., Vaattovaara, P., Viisanen, Y., Vrtala, A., Wagner, P. E., Weingartner, E., Wex, H., Wimmer, D., Carslaw, K. S., Curtius, J., Donahue, N. M., Kirkby, J., Kulmala, M., Worsnop, D. R., and Baltensperger, U.: Oxidation products of biogenic emissions contribute to nucleation of atmospheric particles, Science, 344, 717–721, 2014.

Rose, C., Sellegri, K., Asmi, E., Hervo, M., Freney, E., Colomb, A., Junninen, H., Duplissy, J., Sipilä, M., Kontkanen, J., Lehtipalo, K., and Kulmala, M.: Major contribution of neutral clusters to new particle formation at the interface between the boundary layer and the free troposphere, Atmos. Chem. Phys., 15, 3413–3428, doi:10.5194/acp-15-3413-2015, 2015.

Schobesberger, S., Junninen, H., Bianchi, F., Lonn, G., Ehn, M., Lehtipalo, K., Dommen, J., Ehrhart, S., Ortega, I. K., Franchin, A., Nieminen, T., Riccobono, F., Hutterli, M., Duplissy, J., Almeida, J., Amorim, A., Breitenlechner, M., Downard, A. J., Dunne, E. M., Flagan, R. C., Kajos, M., Keskinen, H., Kirkby, J., Kupc, A., Kuerten, A., Kurten, T., Laaksonen, A., Mathot, S., Onnela, A., Praplan, A. P., Rondo, L., Santos, F. D., Schallhart, S., Schnitzhofer, R., Sipila, M., Tome, A., Tsagkogeorgas, G., Vehkamaki, H., Wimmer, D., Baltensperger, U., Carslaw, K. S., Curtius, J., Hansel, A., Petaja, T., Kulmala, M., Donahue, N. M., and Worsnop, D. R.: Molecular understanding of atmospheric particle formation from sulfuric acid and large oxidized organic molecules, P. Natl. Acad. Sci. USA, 110, 17223–17228, 2013.

Sipilä, M., Berndt, T., Petäjä, T., Brus, D., Vanhanen, J., Stratmann, F., Patokoski, J., Mauldin, R. L., Hyvärinen, A.-P., Lihavainen, H., and Kulmala, M.: The role of sulfuric acid in atmospheric nucleation, Science, 327, 1243–1246, 2010.

Sogacheva, L., Hamed, A., Facchini, M. C., Kulmala, M., and Laaksonen, A.: Relation of air mass history to nucleation events in Po Valley, Italy, using back trajectories analysis, Atmos. Chem. Phys., 7, 839–853, doi:10.5194/acp-7-839-2007, 2007.

Spracklen, D. V., Carslaw, K. S., Kulmala, M., Kerminen, V.-M., Mann, G. W., and Sihto, S.-L.: The contribution of boundary layer nucleation events to total particle concentrations on regional and global scales, Atmos. Chem. Phys., 6, 5631–5648, doi:10.5194/acp-6-5631-2006, 2006.

Tammet, H. and Kulmala, M.: Simulation tool for atmospheric aerosol nucleation bursts, J. Aerosol Sci., 36, 173–196, 2005.

Vanhanen, J., Mikkilä, J., Lehtipalo, K., Sipilä, M., Manninen, H. E., Siivola, E., Petäjä, T., and Kulmala, M.: Particle size magnifier for nano-CN detection, Aerosol Sci. Tech., 45, 533–542, 2011.

Wang, M. and Penner, J. E.: Aerosol indirect forcing in a global model with particle nucleation, Atmos. Chem. Phys., 9, 239–260, doi:10.5194/acp-9-239-2009, 2009.

Weber, R. J., Marti, J. J., McMurry, P. H., Eisele, F. L., Tanner, D. J., and Jefferson, A.: Measurements of new particle formation and ultrafine particle growth rates at a clean continental site, J. Geophys. Res., 102, 4375–4385, 1997.

Xiao, S., Wang, M. Y., Yao, L., Kulmala, M., Zhou, B., Yang, X., Chen, J. M., Wang, D. F., Fu, Q. Y., Worsnop, D. R., and Wang, L.: Strong atmospheric new particle formation in winter in urban Shanghai, China, Atmos. Chem. Phys., 15, 1769–1781, doi:10.5194/acp-15-1769-2015, 2015.

Yli-Juuti, T., Nieminen, T., Hirsikko, A., Aalto, P. P., Asmi, E., Hõrrak, U., Manninen, H. E., Patokoski, J., Dal Maso, M., Petäjä, T., Rinne, J., Kulmala, M., and Riipinen, I.: Growth rates of nucleation mode particles in Hyytiälä during 2003–2009: variation with particle size, season, data analysis method and ambient conditions, Atmos. Chem. Phys., 11, 12865–12886, doi:10.5194/acp-11-12865-2011, 2011.

Yu, F. and Turco, R.: Ultrafine aerosol formation via ionmediated nucleation, Geophys. Res. Lett., 27, 883–886, 2000.

ACPD
15, 33077–33119, 2015

High concentrations of sub-3 nm clusters and frequent new particle formation

J. Kontkanen et al.

Yu, F. and Turco, R.: Case studies of particle formation events observed in boreal forests: implications for nucleation mechanisms, Atmos. Chem. Phys., 8, 6085–6102, doi:10.5194/acp-8-6085-2008, 2008.

Yu, F., Luo, G., Bates, T. S., Anderson, B., Clarke, A., Kapustin, V., Yantosca, R. M., Wang, Y., and Wu, S.: Spatial distributions of particle number concentrations in the global troposphere: simulations, observations, and implications for nucleation mechanisms, J. Geophys. Res., 115, D17205, doi:10.1029/2009JD013473, 2010.

Yu, H., Kanawade, V. P., You, Y., Hallar, A. G., Mccubbin, I. B., Chirokova, G., Sedlacek, A. J., Springston, S. R., Wang, J., Mc-Graw, R. L., Mikkila, J., and Lee, S. H.: Sub-3 nm particles observed at the coastal and continental sites in the United States, J. Geophys. Res.-Atmos., 119, 860–879, doi:10.1002/2013JD020841, 2014.

Yu, H., Zhou, L. Y., Dai, L., Shen, W. C., Zheng, J., Ma, Y., and Chen, M. D.: Nucleation and growth of sub-3 nm particles in the polluted urban atmosphere of a megacity in China, Atmos. Chem. Phys. Discuss., 15, 18653–18690, doi:10.5194/acpd-15-18653-2015, 2015.

Zhang, R., Khalizov, A., Wang, L., Hu, M., and Xu, W.: Nucleation and growth of nanoparticles in the atmosphere, Chem. Rev. E, 112, 1957–2011, 2012.

ACPD
15, 33077–33119, 2015

Table 1. Growth rates of particles during NPF events. The median values and the range from 5- to 95-percentile are shown. The growth rates were determined from the positive ion size distributions measured with the NAIS.

Size range	Growth rate [$nm\,h^{-1}$]
1.5–3.0 nm	4.3 (1.0–10.0)
3.0–7.0 nm	6.0 (2.6–12.9)
7.0–20.0 nm	7.2 (3.8–13.8)

ACPD
15, 33077–33119, 2015

Table 2. The formation rates of all clusters and ions during NPF events. The median values and the range from 5- to 95-percentile are shown. The formation rates of all clusters at 1.6 nm were determined from PSM data. The formation rates of ions at 1.6 nm and all clusters and ions at 2 nm were determined from NAIS data.

Size	Clusters	Formation rate [$cm^{-3}\,s^{-1}$]
1.6 nm	All clusters	45 (23–53)
1.6 nm	Positive ions	0.19 (0.09–0.32)
1.6 nm	Negative ions	0.06 (0.03–0.08)
2.0 nm	All clusters	6.8 (2.7–38.5)
2.0 nm	Positive ions	0.12 (0.05–0.25)
2.0 nm	Negative ions	0.08 (0.03–0.19)

ACPD
15, 33077–33119, 2015

High concentrations of sub-3 nm clusters and frequent new particle formation

J. Kontkanen et al.

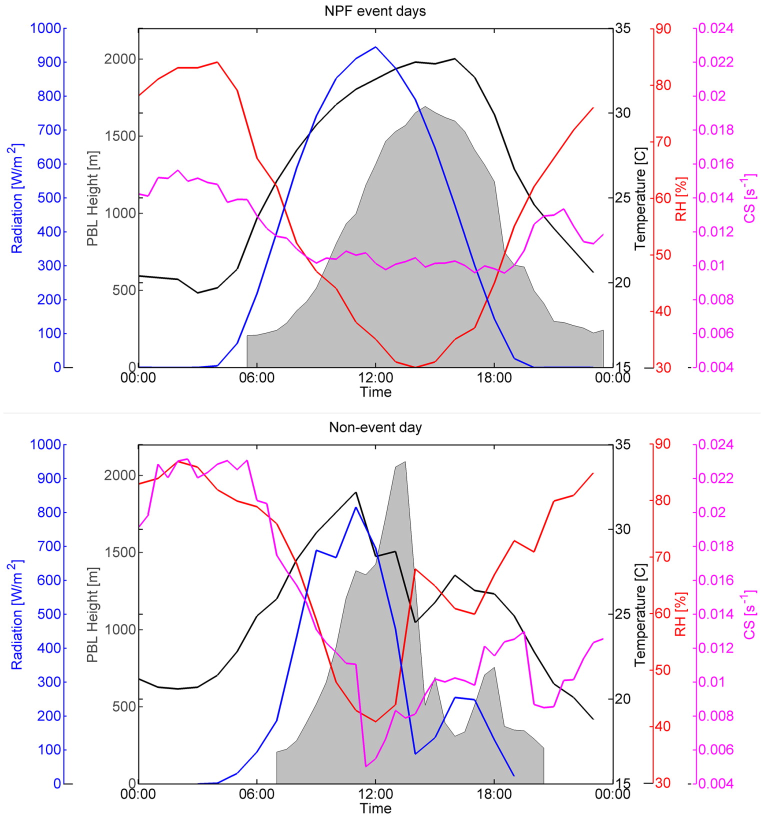

Figure 1. The median diurnal variation of global radiation (blue line), PBL height (grey area), temperature (black line), relative humidity (RH; red line) and condensation sink (CS; magenta line) on NPF event days and on the only non-event day (6 July 2012). Time is UTC + 1 h.

ACPD
15, 33077–33119, 2015

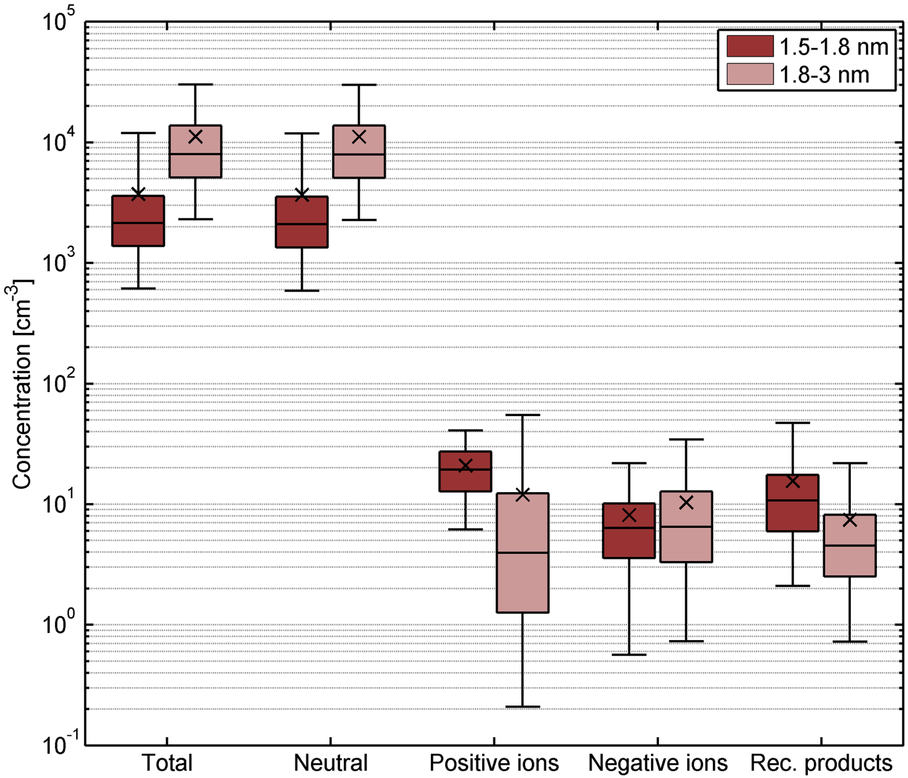

Figure 2. The median concentration of all clusters, neutral clusters, positive ions, negative ions and recombination products in the two size bins (1.5–1.8 nm and 1.8–3.0 nm). The edges of the boxes show the 25- and 75-percentiles and the centers of the boxes represent the median values. The mean values are presented with black crosses. The error bars show the 5- and 95-percentile values.

ACPD
15, 33077–33119, 2015

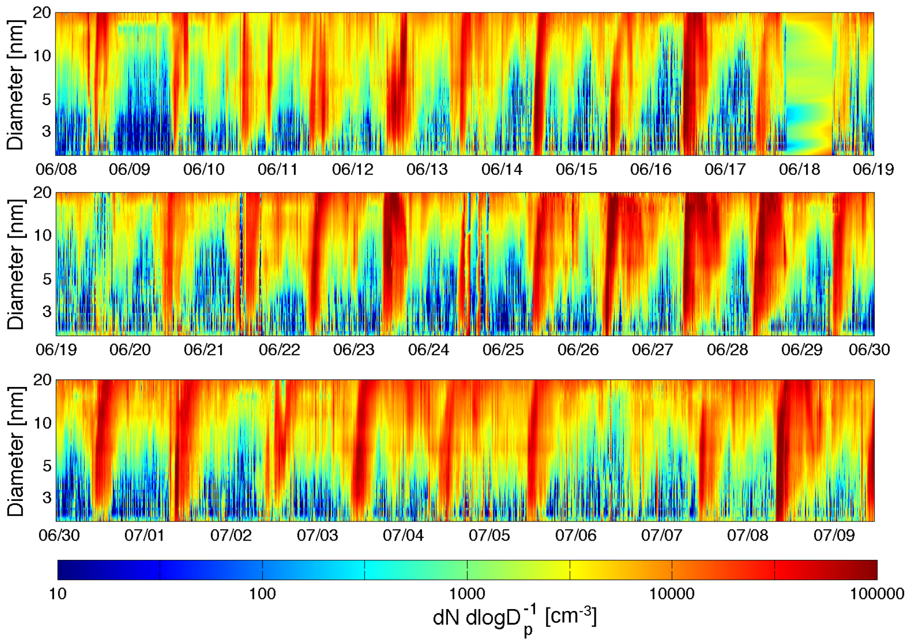

Figure 3. Time series of particle size distribution measured with the NAIS during 8 June–9 July 2012 in San Pietro Capofiume.

ACPD
15, 33077–33119, 2015

High concentrations of sub-3 nm clusters and frequent new particle formation

J. Kontkanen et al.

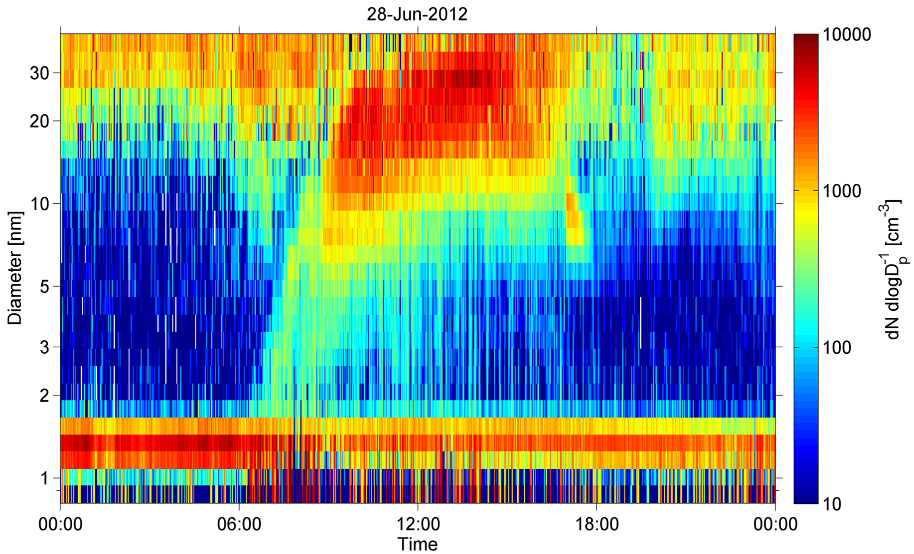

Figure 4. The size distribution of positive ions on a typical new particle formation event at the San Pietro Capofiume station (28 June 2012).

ACPD
15, 33077–33119, 2015

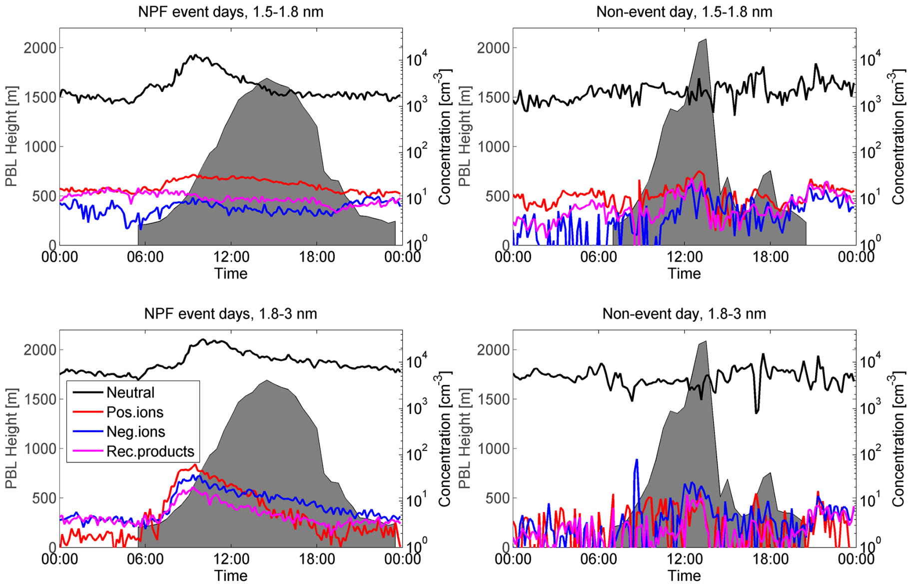

Figure 5. The median diurnal variation of the concentrations of neutral clusters (black line), positive ions (red line), negative ions (blue line) and recombination products (magenta line) on NPF event days and on the only non-event day (6 July 2012). In addition, the PBL height is shown in grey. Time is UTC + 1 h.

ACPD
15, 33077–33119, 2015

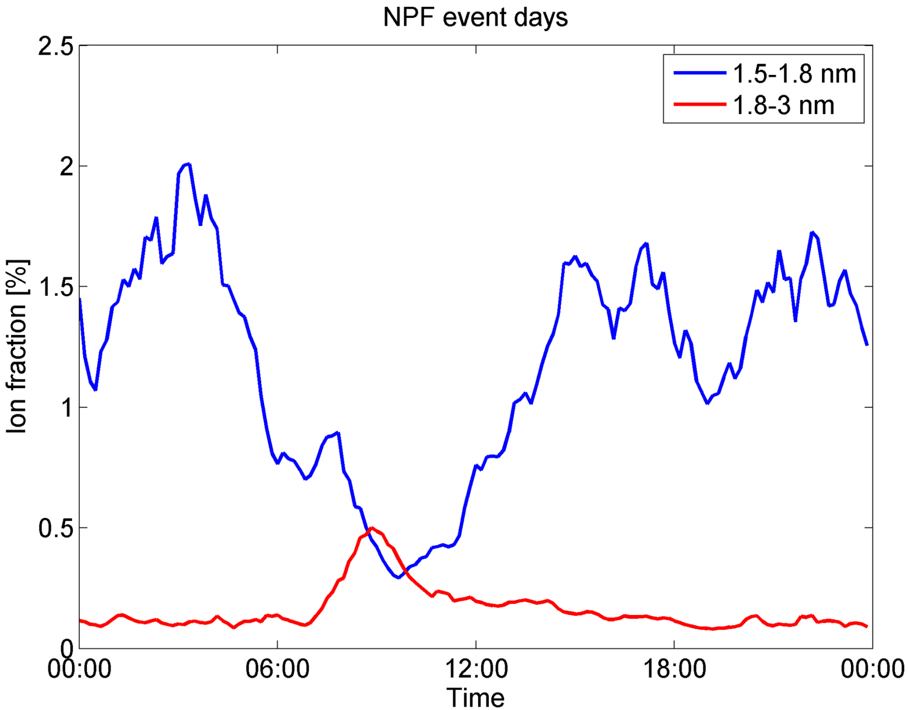

Figure 6. The median diurnal variation of the fraction of ions of all clusters in the size bins of 1.5–1.8 nm (blue line) and 1.8–3.0 nm (red line) on NPF event days. Time is UTC + 1 h.

ACPD
15, 33077–33119, 2015

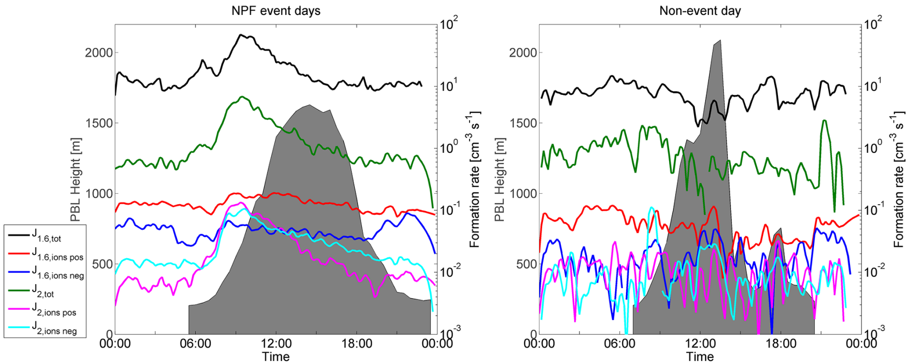

Figure 7. The median diurnal variation of the cluster formation rates at 1.6 and 2 nm on NPF event days and on the only non-event day (6 July 2012). The PBL height is shown in grey. In the subscripts numbers refer to the size of the cluster in nanometers and "tot" refers to total clusters, "pos" to positive ions and "neg" to negative ions. Time is UTC + 1 h.

ACPD
15, 33077–33119, 2015

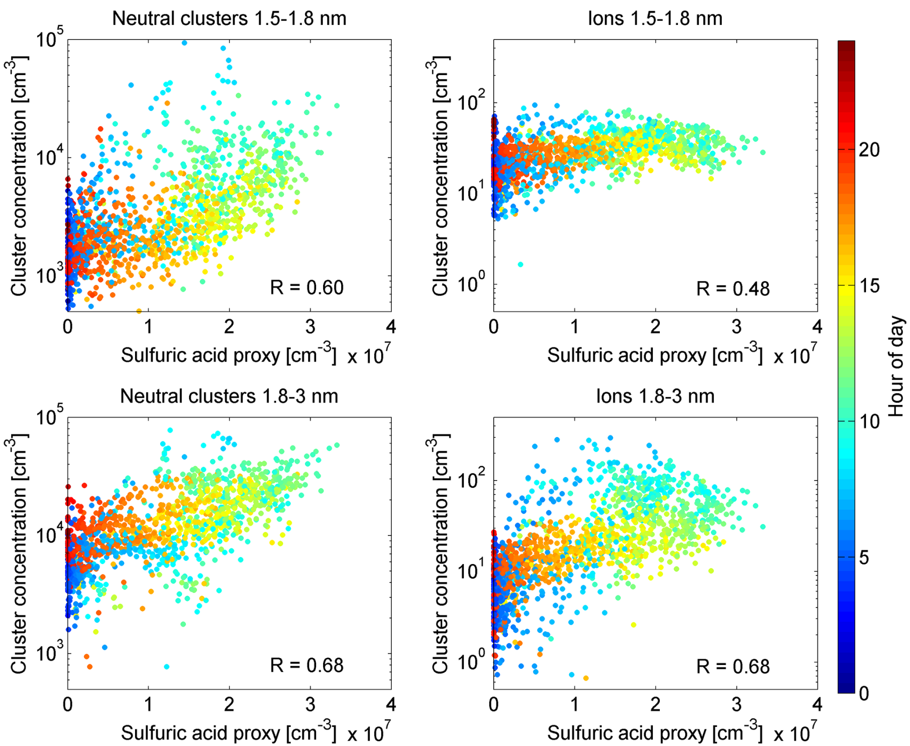

Figure 8. The correlation between the neutral and charged 1.5–1.8 nm and 1.8–3.0 nm clusters and sulfuric acid proxy. The color bar shows the hour of day. The correlation coefficients (R) are presented in the figures.

ACPD
15, 33077–33119, 2015

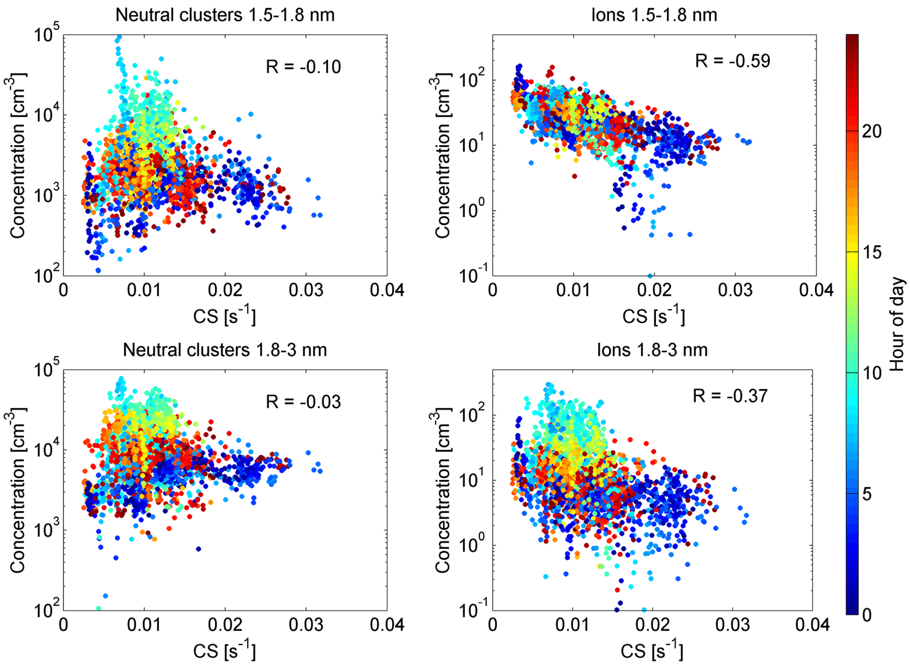

Figure 9. The correlation between the neutral and charged 1.5–1.8 nm and 1.8–3.0 nm clusters and condensation sink (CS). The color bar shows the hour of day. The correlation coefficients (R) are presented in the figures.

ACPD
15, 33077–33119, 2015

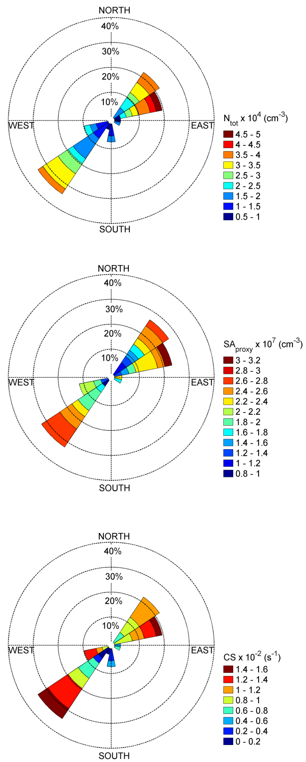

Figure 10. Air mass arrival directions and their relation to the total concentration of 1.8–3.0 nm clusters (N_{tot}), sulfuric acid proxy (SA_{proxy}) and condensation sink (CS) in San Pietro Capofiume around midday (between 10 a.m. and 2 p.m.). The length of the sectors illustrates how frequently an air mass trajectory arrived from that direction. The color of the sectors shows the value of the measured variable in San Pietro Capofiume at the arrival time of the trajectory.

ACPD
15, 33077–33119, 2015